

1 **Recording of multiple lake-marsh**  
2 **paleoenvironments during the middle Holocene in**  
3 **the Quebrada del Toro, NW Argentina**

4  
5 **Juan G. VEIZAGA SAAVEDRA<sup>1</sup>, María Cristina SÁNCHEZ<sup>1</sup>, Olga MARTÍNEZ<sup>2</sup>, Heiko PINGEL<sup>3</sup>, Claudio G.**  
6 **DE FRANCESCO<sup>4</sup>**

7  
8 <sup>1</sup>Cátedra de Estratigrafía y Geología Histórica, Universidad Nacional de Salta, Avda. Bolivia 5150, 4400 Salta

9 <sup>2</sup>Facultad de Ciencias Naturales, Herbario MCNS, Instituto de Bio y Geociencias del NOA (IBIGEO-CONICET)

10 <sup>3</sup>Institut für Geowissenschaften, Universität Potsdam, 14476 Potsdam, Germany

11 <sup>4</sup>Instituto de Investigaciones Marinas y Costeras (IIMyC), CONICET, UNMdP, Mar del Plata, Argentina

12

13 Corresponding Author: Juan Gonzalo Veizaga Saavedra. [juangveizaga@gmail.com](mailto:juangveizaga@gmail.com)

14

15 Editor: Francisco Córdoba

16 Enviado: 10 de agosto de 2020

17 Aceptado: 23 de mayo de 2021

18

19 **ABSTRACT**

20 Quaternary lake systems have developed in many Andean intermontane valleys in northwestern  
21 Argentina in association with landslides, rock avalanches, and the development of large alluvial fans,  
22 caused either by tectonics, climate change, and/or increased rainfall. At the El Candado location, in the  
23 narrow, southern sector of the Quebrada del Toro (Salta Province, Argentina), fine-grained sedimentary  
24 deposits are recognized, which, based on their sedimentological and paleontological characteristics, are  
25 interpreted as the sedimentary infill of shallow lakes-marshes that were generated by the development  
26 of large alluvial fans that dammed the Río Toro. Based on AMS <sup>14</sup>C dating of gastropod shells and  
27 organic matter (ca. 8-4.8 ka), this region experienced multiple lacustrine-marsh paleoenvironments  
28 during the middle Holocene. Pollen analysis and paleobotanical investigations of these deposits suggest  
29 that the accumulation of the lake sediments occurred under relatively humid conditions that alternated  
30 with semi-arid periods as is typical for the Andean Holocene.

31

32 **Keywords:** Quaternary, Central Andes, Paleoflora, Molluscs, Paleoclimate

33

34 **RESUMEN**

35 *Registro de múltiples episodios lacustre-palustres durante el Holoceno medio en la Quebrada del Toro,*

36 *noroeste argentino*

37 En el noroeste argentino durante el Cuaternario se desarrollaron sistemas lacustres asociados con  
38 deslizamientos, avalanchas de roca y desarrollo de grandes abanicos aluviales, generados por la  
39 actividad tectónica andina, los cambios climáticos y/o lluvias extraordinarias. En la localidad de El  
40 Candado, tramo inferior de la Quebrada del Toro (provincia de Salta, Argentina), se reconocen  
41 afloramientos pelíticos que son interpretados en base a sus características sedimentológicas y  
42 paleontológicas como acumulaciones lacustres-palustres someras. Estos depósitos se habrían producido  
43 a partir de la instalación de un ambiente lacustre-palustre como consecuencia del desarrollo de un gran  
44 abanico aluvial que obstruyó al río Toro. La sedimentación ocurrió durante el Holoceno medio de  
45 acuerdo con la datación de gasterópodos y materia orgánica que arrojaron edades entre 8-4.8 ka. Según  
46 los restos paleobotánicos y palinológicos así como los atributos sedimentológicos, la acumulación  
47 ocurrió en ambientes lacustre-palustre temporarios, somero bajo condiciones húmedas que habría  
48 alternado con las condiciones paleoclimáticas áridas y secas que caracterizaron al Holoceno medio de  
49 esta región de los Andes Centrales.

50

51 Palabras clave: Cuaternario, Andes Centrales, Paleoflora, Moluscos, Paleoclima

52

## 53 INTRODUCTION

54 During the late Pleistocene- early Holocene, transient mountain lakes were formed in various locations  
55 and settings throughout the arid and semi-arid regions of northwestern Argentina associated with  
56 landslides, seismic events or the development of large alluvial fans during periods of increased rainfall  
57 (Hermanns and Strecker 1999, Wayne 1999, Bookhagen et al. 2001, Trauth et al. 2003, Colombo 2005,  
58 Hermanns et al. 2004, Savi et al. 2016). As a result, many intermontane river valleys have preserved  
59 remnants of lacustrine deposits, often recognizable by their typical ochre to yellow colors. One of these  
60 valleys is the Quebrada del Toro in the Eastern Cordillera of the southern Central Andes (Fig. 1). Along  
61 its main river (Río Toro), discontinuous outcrops of 10 to 50 m thick Quaternary lake deposits have  
62 been recognized that are laterally and vertically related to alluvial-fluvial accumulations of the same  
63 age (Robinson et al. 2005, Álvarez et al. 2012).

64 Sedimentary deposits of intermontane paleolakes are important but relatively rare repositories of  
65 proxy material to investigate and reconstruct past environmental conditions and their changes over time  
66 in orogenic landscapes (e.g. Trauth et al. 2000, Hermanns et al. 2004, Colombo et al. 2009, Piovano et  
67 al. 2014). Among these proxy data, sedimentary and geochemical compositions, floral and faunal fossil  
68 remains, and often pollen, are used to provide a snapshot of the paleoenvironment including climatic  
69 and biotic conditions during lake deposition (e.g. Garralla et al. 2001, De Francesco et al. 2007, 2009).  
70 For that matter, datable materials (e.g. organic carbon, fossils, volcanic ash) are just as helpful as their  
71 prominent appearance in the landscape. Of particular interest in this study are late Quaternary

72 environmental changes in the Argentine Andes, which remain enigmatic (e.g. Tchilinguirian and  
73 Morales 2013, Tiner et al. 2018) due to various aspects such as the availability of suitable data and the  
74 complex interactions between climate systems and mountain topography (e.g. Strecker et al. 2007,  
75 Bookhagen and Strecker 2012, Barnes et al. 2012).

76 Our study focusses on the lower section of the Río Toro where the valley is considerably narrow  
77 and the adjacent mountain flanks are steep (Fig. 2). Recent studies showed that these slopes are unstable  
78 and prone to failure and generation of debris flows (Olen et al. 2020), while catchment-wide erosion  
79 rates from the flanking tributaries are high (Tofelde et al. 2018). As a consequence, at the outlets of  
80 these tributaries, many wide and asymmetric alluvial fans have developed, characterized by fan areas  
81 between 0.2 and 2 km<sup>2</sup> (on average 1 km<sup>2</sup>), a surface slope of 5° to 10°, and a thickness of 10-15 m  
82 (Veizaga Saavedra 2012). Due to relatively large amounts of sediment added to the main river, active  
83 alluvial fans have often influenced the dynamics of the Río Toro by altering the local base level, which  
84 led to reduced run-off gradients, upstream aggradation, and potentially the damming of the river to form  
85 transient lake systems (Sánchez et al. 2005, 2010). Similar observations have been made throughout the  
86 Argentine Andes for the late Pleistocene-Holocene (e.g. Colombo 2005, Colombo et al. 2005, 2009,  
87 Pingel et al. 2013, Savi et al. 2016, May and Soler 2011).

88 At the confluence of the El Candado stream and the Río Toro (El Candado site) (Figs. 2, 3), we  
89 document several outcrops that show lacustrine beds with an average thickness of 2.5 m that are  
90 interbedded and interdigitated with alluvial fan sediments (Fig. 4). Despite their potential to provide  
91 valuable information on past climate changes, these deposits have not been studied in detail. Therefore,  
92 we present new chronostratigraphic (AMS <sup>14</sup>C), sedimentological, mineralogical, geochemical, and  
93 paleontological data for preserved lacustrine beds from five stratigraphic sections along the lower  
94 section of the Quebrada del Toro and place them into a refined stratigraphic and paleoclimatic context.  
95 Based on this data, we show that during the middle Holocene this region experienced multiple lake-  
96 marsh episodes, which are most likely related to the development of an alluvial fan at the confluence of  
97 the El Candado stream and the Río Toro.

## 99 GEOLOGICAL AND CLIMATIC SETTING

100 The studied El Candado area (ca. 24.8°S, 65.6°W) is located near the confluence of the El Candado  
101 stream and the Río Toro in the intermontane Quebrada del Toro, which is an integral part of the Eastern  
102 Cordillera morphotectonic domain (Fig. 1, 2). The Quebrada del Toro is a fault-bounded intermontane  
103 valley delimited by approximately NNW-SSE striking, bivergent reverse faults and associated mountain  
104 ranges (Marrett et al. 1994, and references therein). More specifically, the El Candado area is located  
105 in a narrow, structurally controlled basement gorge through which the Río Toro exits the valley to the

106 south and along which several minor tributaries (e.g. El Candado and El Alisal streams) and one major  
107 tributary (Río Capillas) enter the river valley (Fig. 2). A major fault crossing the valley in the study area  
108 is the east-dipping Incamayo Fault (Fig. 2). Adjacent mountain ranges to the east and west exceed 3,000  
109 m a.s.l. and their valley flanking slopes average around 30° (e.g. Tofelde et al. 2018). The basement  
110 rocks exposed in the study area mainly comprise Neoproterozoic to early Cambrian meta-sediments of  
111 the Puncoviscana Formation (Turner 1960) that are unconformably overlain by mainly fluvial and  
112 alluvial Quaternary sediments (Fig. 3). The latter comprise occasional intercalation of lacustrine beds  
113 (this study).

114 The eastern flanks of the southern Central Andes of Argentina are characterized by pronounced  
115 orographic rainfall gradients (Fig. 1b, Bookhagen and Strecker 2008). Water vapor transport from the  
116 Atlantic Ocean and Amazon Basin is mainly governed by the South American Monsoon system  
117 (SAMS), in which the South American low-level jet (SALLJ) funnels air masses southward along the  
118 Andes into (sub-) tropical South America (Castino et al. 2016, Vera et al. 2006). The Quebrada del Toro  
119 receives rainfall ranging from ~900 mm/yr at the outlet to <200 mm/yr in the interior of the  
120 intermontane basin (Figure 1). Moisture supplied to the Central Andes has varied significantly over the  
121 past several tens of thousands of years (Baker and Fritz 2015). Variability in the intensity of SAMS  
122 precipitation on precessional timescales (21 kyr) has been documented by paleo-lake studies on the  
123 Puna Plateau of Argentina and Chile and the Bolivian Altiplano (Bobst et al. 2001, Godfrey et al. 2003,  
124 Fritz et al. 2010, Fritz et al. 2004, Placzek et al. 2006).

125 On interannual timescales, El Niño/Southern Oscillation (ENSO) is the main source of variability  
126 in precipitation and circulation over South America, this system would have influenced the South  
127 American continent during the Quaternary in a dissimilar way (Markgraf et al. 1986, Villagrán and  
128 Varela 1990, Markgraf and Seltzer 2001, Villa Martínez et al. 2003). Many studies have shown that  
129 during El Niño events, precipitation is suppressed over central-eastern Brazil and enhanced over  
130 southeastern South America (southern Brazil, Uruguay, and northern Argentina), while opposite  
131 anomalies are observed during La Niña events (Grimm 2011). Also, the subtropical rainfall anomalies  
132 during El Niño are related to a stronger SALLJ and enhanced pole ward moisture transport to  
133 southeastern South America (Zhou and Lau 2001), therefore the interannual variability of the jet's  
134 strength and frequency is significantly modulated by the El Niño Southern Oscillation, especially during  
135 spring (Montini et al. 2019).

136

## 137 **METHODOLOGY**

138 We used traditional sedimentological and stratigraphic techniques to characterize five individual  
139 alluvial stratigraphic sections containing intercalated lacustrine beds (El Alto, La Cirila, Los Cardones,

140 El Candado West and El Candado sections, Fig. 2) using the lithofacies classification of Miall (1996)  
141 and the lake classification of Fregenal Martinez et al. (2010). In addition, we collected 11 bulk lake-  
142 sediment samples from the El Candado section for geochemical analyses by energy-dispersive X-ray  
143 spectrometry (EDS). For this purpose, samples were air-dried, gold-coated, and analyzed using an FEI  
144 Quanta 200 SEM microscope and an EDAX Phoenix 40 (acceleration voltage 20 keV, spot size 3 to 4  
145 mm) at the Faculty of Engineering, La Plata, Argentina. Each sample was studied at varying  
146 magnification up to 25,000 to determine the major and minor mineralogical components. In addition,  
147 clay mineral compositions were determined by EDS and their morphologies were identified by scanning  
148 electron microscopy (SEM).

149 Four samples were analyzed by X-ray diffractometry (XRD) to determine the mineral composition  
150 of lake sediments. Samples were gently ground with a rubber mortar and repeatedly washed in distilled  
151 water until deflocculation occurred. The <2 mm fraction was separated by suspension and gravity  
152 decantation, and oriented samples were prepared on glass slides. Clay mineralogy was determined from  
153 diffraction patterns obtained using samples that were air-dried, solvated with ethylene glycol, and  
154 heated to 550°C for 2 hours (Brown and Brindley, 1980). The diffractograms were performed in an  
155 X'Pert PRO model X PANalytical (CIG) diffractometer, using Cu/Ni radiation and 40 kV and 40 mA  
156 generation settings.

157 The weighting (semi-quantitative) of the minerals present in the total rock was carried out from the  
158 intensity of the main peak for each mineral (Schultz 1964, modified with own standards; Moore and  
159 Reynolds 1997). The estimation of the mineralogical components has a methodological error ca. 10%.  
160 The semi-quantitative estimates of the relative concentrations of clay minerals were based on the peak  
161 area method following the Biscaye (1965) methodology. The response of mineral species to  
162 sedimentation depends on the shape of the particles (Pierce and Siegel 1969). For that reason, each  
163 mineral proportion is not directly proportional to the defined areas. The relative percentages of each  
164 clay mineral were determined by applying empirical factors (Moore and Reynolds 1997).

165 In the El Alto, La Cirila, and Los Cardones sections, we collected fossil plant remains that were  
166 identified at the Herbarium of the National University of Salta. Observations, measurements and  
167 photographs were made using an Optika SZM-LED2 stereoscopic magnifying glass with a Motic-  
168 MotiCAM BTU10 camera and a JEOL JSM6480LV scanning electron microscope.

169 To determine the correlation of the lake deposits in the El Candado locality with other recognized  
170 lacustrine deposits, we dated gastropod shells and organic matter using the AMS <sup>14</sup>C method. The  
171 samples were extracted and cleaned in the mineral separation laboratories of the University of Potsdam  
172 (Germany) and then sent to the Radiocarbon Laboratories in Poznan (Poland) for radiocarbon analysis.

173 For the mapping of Quaternary deposit within the southern sector of the Quebrada del Toro and a

174 2D reconstruction of the paleotopography of the abandoned fan surface (Fig. 2), we used a combination  
175 of field- and satellite-based mapping and DEM-processing tools in QGIS software and TopoToolbox,  
176 a Matlab-based toolset for topographic analysis (Schwanghart and Kuhn 2010). The base for these  
177 analyses is a TanDEM-X digital elevation model (DEM) with 12 m spatial resolution (<https://gdk.gdi->  
178 [de.org/geonetwork/srv/api/records/5eecd4c-de57-4624-99e9-60086b032aea](https://gdk.gdi-de.org/geonetwork/srv/api/records/5eecd4c-de57-4624-99e9-60086b032aea)).

179

## 180 RESULTS

### 181 Stratigraphy and sedimentology

182 Eight lithofacies of alluvial-fluvial (gravel: Gmc, Gm, Gng, Gig and sand: Sm, St, Sr, Sh) and two  
183 lithofacies of lacustrine origin (clay: Clm and silt: Lm) have been defined. A summary of lithofacies  
184 and interpretations used in this study is shown in Table 1.

185 (1) In general, the greenish-grey gravel facies (G) are poorly sorted and consist of medium to coarse  
186 gravel that are either, clast-supported (Gmc) or matrix-supported (Gm), with normal (Gng) or inverse  
187 (Gig) gradation (Fig. 6a). Clasts exclusively meta-graywackes, slates, and phyllites from Puncoviscana  
188 Formation are angular to subangular, oblate, prolate, and laminar. The matrix is composed of silts to  
189 silty clay and sand. The stratification is diffuse, tabular and lenticular, with erosive or planar base and  
190 the thickness of the beds is between 0.5 and 1 m.

191 (2) Sand facies (S) are represented by moderately sorted, medium to coarse, and sub-rounded sand  
192 with either planar-cross lamination (St), massive appearance (Sm), parallel lamination (Sh) or with  
193 current ripple-lamination (Sr). The stratification is tabular, with a planar base and top and the thickness  
194 of the beds is between 0.5 and 1 m. Occasional fine-grained, lenticular sandy levels are 3 to 5 cm thick  
195 with planar and parallel lamination (Sh) are interbedded with pelitic facies and contain abundant  
196 carbonate cement. In addition, these sandy beds contain oxidized parts.

197 (3) Two pelitic facies have been identified: massive silt (Lm) and massive clay (Clm). Both form  
198 tabular beds with sharp and flat base between 1 and 2.5 m thick (Fig. 6b). The clay levels contain  
199 abundant black and reddish-ocher plant remains, gastropod shells, and show abundant bioturbation.

200 These lithofacies were grouped into two facies associations that are identified in some levels of the  
201 stratigraphic sections considered (Fig. 5):

202 (1) Facies association A-F: It consists of the aggradation of gravel bodies (Gmc and Gm) mantiform,  
203 tabular, up to 2 m thick, with poor selection and poor textural maturity, generally massive, although at  
204 the finest levels a certain normal gradation is recognized. The sedimentary features of the G lithofacies  
205 such as the presence of fine interstitial matrix, the angular and monomictic character of the individuals,  
206 the absence of stream structures and the chaotic fabric suggest a massive flow of debris along a very  
207 steep slope during episodes of large discharge of water and sediment. Thus, these facies would have

208 been deposited by high-kinetic energy, high-density and high-viscosity flows of the debris flow type  
209 (Coussot and Meunier 1996, Blikra and Nemeč 1998). On the other hand, if it considers: 1) the slope  
210 of the alluvial fans (15° average; Veizaga Saavedra 2012), 2) the proximity of the source areas and 3)  
211 the high availability of material to be mobilized due to the nature of the source areas, it is possible that  
212 the fine-grained G lithofacies could be the result of intermediate flows, between hyper-concentrates and  
213 fluids (Suriano and Limarino 2009).

214 The Gmc and Gm facies grade vertically and laterally to lithofacies composed of tabular beds of  
215 coarse to medium massive sand (Sm) with abundant plant remains. These are interpreted as sheet flood  
216 deposits generated by hyper-concentrated flows (Blair and McPherson 1994) produced by low-  
217 frequency and high-intensity rainfall (Gutiérrez et al. 1988) that are typical of the Holocene of the arid  
218 to semi-arid region of the Central Andes (Tofelde et al. 2017).

219 In the El Candado West and El Candado sections, lenticular levels of medium sand with planar-  
220 cross lamination (St) are recognized associated with the Sm facies (Fig. 5). These are the result of the  
221 migration of small sand waves under the influence of fluid, tractional and unidirectional currents  
222 (Collinson and Thompson 1989) that occur when the intensity of precipitation is greater than the  
223 infiltration capacity of the soil (Gutiérrez Elorza 2001).

224 (2) Facies association of L-M facies: In all the studied sections, it is characterized by monotonous  
225 clastic successions of massive clays with desiccation cracks. In the El Candado and El Candado West  
226 sections (Fig. 5), tabular levels of massive silt are interbedded. In the five sections considered, fine  
227 tabular beds of fine sand, with a planar to wavy base, with parallel lamination (Sh) and ripple lamination  
228 (Sr) are intercalated. The pelites contain abundant black and reddish-ocher plant remains with  
229 bioturbation (Fig. 6b) and remains of gastropod shells (Fig. 7a-b) in the sections of La Cirila, Los  
230 Cardones and El Candado.

231 The sedimentological characteristics of the Clm/Lm association suggest that sedimentation occurred  
232 under conditions of low flow regime and with a predominance of suspension-fallout processes in a  
233 water body. Among the pelitic beds, tabular levels of fine sand with carbonate cement (Sh/Sr) are  
234 recognized that would be linked to sporadic tractive flows produced by the entry of a river course into  
235 a lentic water body (Spalletti 2001). This means that the El Candado lake levels described in this study  
236 would have been shallow, ephemeral, and vegetated as suggested by sedimentary structures and fossil  
237 content.

238

### 239 **Mineralogy and geochemistry**

240 The samples analyzed are homogeneous and display small compositional variations; contents of major  
241 elements were determined: O (44-48%), Si (23-32%), Al (5-12%), minor amounts of Fe (4-9%), K (1-

242 5%), Ca (1-3%) and Mg (1-2%) (Fig. 8a-b). Likewise, Na, Co, Ba, Cl, I, P and Mn were identified in  
243 trace concentrations. It should be noted that the samples bearing abundant plant and gastropod remains  
244 showed high values of K (3.61%), Ca (2.73%), Mg (1.78%) and Na (1.29%). The mineralogy of lake  
245 sediments is characterized by quartz (50-75%), plagioclase (5-15%), potassium feldspar (1-5%) and  
246 clay minerals (15-30%) (Fig. 8). Clay mineral assemblages defined by X-ray diffraction consist of illite  
247 (45-60%), smectite (5-20%), illite/smectite mixed-layer (5%), chlorite (20-30%), and kaolinite (5%)  
248 (Fig. 8c-d). SEM analyses reveal that illite show as high fragmented clays with variable size, irregular  
249 borders and without a preferential order. Their EDS analysis show in descending order Si, Al, Na, Mg,  
250 K, and Fe (Fig. 8a). Smectite shows as curled flakes with open-air voids having small interfacial zones  
251 and as flaky particle morphology (Fig. 8b). EDS shows that Si is the major cation, followed by Al, Na,  
252 K, Mg and Fe in order of abundances (Fig. 8b), and in some cases, minor Ca.

253

#### 254 **Paleontology**

255 In the Los Cardones section, a 1.5 m thick level of massive clay is recognized; the paleobotanical record  
256 consists of dicotyledonous remains exhibiting the lignified tissues of a woody plant, in which the growth  
257 rings were preserved, with conducting vessels and the supporting tissue of erect plants. In the La Cirila  
258 section, a 0.9 m thick clay bank bears plant remains of a large leathery leaf in which the veins, petioles  
259 of leaves, leaves of tapered sheets characteristic of grasses, fruit imprints of dicotyledons are identified  
260 and seeds similar to the modern *Aeschynomene* (Fabaceae) (Fig. 7c-h). In 2.5 m thick massive clay and  
261 silt levels of the El Alto section, black and red dicotyledonous remains were collected in which  
262 conducting vessels with secondary growth are recognized.

263 In the La Cirila section, remains of shells of the genus *Biomphalaria* (represented mainly by *B.*  
264 *peregrina*) are recognized (Figs. 7a and b). Shells have an average diameter of 4 mm, they are very  
265 fragmented and exhibit a poor state of preservation, characterized by surface dissolution. Shells have  
266 been dated by AMS  $^{14}\text{C}$  and results indicate that the molluscs and, therefore, the sedimentary deposits  
267 that host them have a middle Holocene age of  $6,440 \pm 40$  cal. years BP (Table 2). In addition, fragments  
268 of indeterminate gastropod shells were collected at different stratigraphic levels. Moreover, organic  
269 matter from the El Alto section has been dated by AMS  $^{14}\text{C}$ , results indicate that the paleontological  
270 remains, and thus the sedimentary deposits they host, are of middle Holocene age:  $8,030 \pm 60$  and  $7,420$   
271  $\pm 80$  cal. years BP for the lower section; and  $4,790 \pm 40$  and  $4,825 \pm 35$  cal. years BP for the upper  
272 section (Table 2).

273 In all sections, samples were collected for palynological analysis at the Palynology Laboratory of  
274 the National University of Jujuy; some samples were productive in the content of palynomorphs. The  
275 assemblage is diverse and consists of pollen types with species of marsh plants (Cyperaceae), terrestrial



276 (Poaceae, Asteraceae, Celtidaceae (*Celtis*), Betulaceae (*Alnus*) and trilete and monolet spores of ferns.

277

### 278 **Geomorphological analyses**

279 Based on our geomorphological analyses of the southern sector of the Quebrada del Toro we were able  
280 to reconstruct the paleotopography of the abandoned/non-active El Candado paleofan surface in 2D.  
281 These analyses show that the paleofan surface is approximately 60 m above the present-day stream (Fig.  
282 2d). At its confluence with the Río Toro, this surface is located at an altitude of 2,000 m above sea level  
283 and must have extended at a similar altitude towards the western flank of the valley. Thus, the upstream  
284 projection of the 2,000 m contour line outlines the maximum extent of a potentially dammed lake  
285 environment.

286 Another intriguing observation from our Río Toro profile analysis is a notable change from a convex  
287 river profile above and a concave profile below the confluence of the Río Capillas (Fig. 2c), where the  
288 main valley floor also widens downstream from less than 100 m near El Candado to up to 450 m near  
289 El Alisal.

290

## 291 **DISCUSSION**

### 292 **Paleoenvironmental interpretation**

293 In the El Candado region, multiple shallow lacustrine-marsh episodes are documented. These lakes had  
294 a maximum area of about 1 km<sup>2</sup> (Fig. 2b) and were hydrologically open according to Collinson's (1978)  
295 classification. Its deposits are exclusively characterized by detrital facies and are vertically related to  
296 alluvial-fluvial systems (Fig. 5).

297 Sedimentation began in marginal positions of the lake (coastal zone; Fregenal Martinez et al. 2010)  
298 with the installation of a fining-upward alluvial system characterized by debris flows. This pattern is  
299 well developed in the El Alto, El Candado West, and El Candado sections (Fig. 5). Towards the center  
300 of the basin, the thickness of the coarse-grained facies is significantly reduced, so that the supralittoral  
301 zone is predominantly characterized by psammitic levels with medium to fine grain sizes (Fregenal  
302 Martinez et al. 2010). These psammitic levels were derived by unconfined flows and are deposited as  
303 massive or parallel laminated beds. In some cases, these beds grade to sand facies with cross-lamination  
304 that corresponds to ephemeral river systems such as flood beds generated during periods of increased  
305 rainfall that would have affected the entire study area.

306 In the middle of the valley, a lacustrine body formed, which is documented by the massive clay  
307 facies (Clm). The periphery of the lake constitutes a mud plain of siltstones (Lm) interstratified with  
308 the massive clays (Clm). These fossiliferous beds show all characteristics of a flooded marsh  
309 environment populated by grasses or poaceae, fabaceae, and shrubs. The suspension-fallout processes

310 would have been interrupted by tractive flows responsible for the accumulation of fine sandstone beds  
311 with carbonate cement and high regime parallel-lamination coinciding with a period of increased  
312 rainfall within the drainage area. Source of the carbonate cement are either Cretaceous limestones of  
313 the Yacoraite Formation (e.g. Marquillas et al. 2005) or reworked material from abundant Quaternary  
314 conglomerates (e.g. Pingel et al. 2020) exposed in the central and upper sections of the Quebrada del  
315 Toro. Finally, in this lake-marsh environment, sedimentological features have been identified that  
316 indicate subaerial exposure by lake level fluctuations: desiccation cracks, discontinuous calcic horizons  
317 (<0.5 cm), oxidized plant remains, suprastratal trace fossils, and vertical bioturbation.

318

### 319 **Mineralogy and geochemistry**

320 Based on similarities in the geochemical and mineralogical composition it is inferred that all the lake  
321 records recognized in the study area would be genetically related during an episode prone to lake  
322 formation. The geochemical composition of lacustrine deposits with abundant plant and gastropod  
323 remains suggest alkaline waters, in line with the lentic water bodies composition, which represents low  
324 or zero flow velocity ( $\leq 0.7$  m/s), low conductivities (0.1-1.7 mS/cm) and relatively high pH values  
325 (7.1-9.4) (De Francesco and Hassan 2009).

326 Clay minerals consist mainly of illite, chlorite, and smectite with small amounts of kaolinite. While  
327 illite and chlorite are the product of low-grade metamorphism and occur mainly in the Puncoviscana  
328 Formation, smectite is formed from chlorite by groundwater interaction under oxidizing conditions (Do  
329 Campo and Nieto 2003). Another smectite source may be the alteration of volcanic glass (Chamley  
330 1997), a very rich source considering the abundance of volcanic deposits in the Quebrada del Toro (e.g.  
331 Molina 2006, Mazzuoli et al. 2008, Vezzoli et al. 2009, 2012, Pingel et al. 2020).

332 Finally, kaolinite may result from alteration of feldspar and mica from the Precambrian to Lower  
333 Paleozoic Tastil batholith (Kilmurray and Igarzábal 1971), the above mentioned volcanics from the  
334 central and southern Quebrada del Toro, and the weathering of micaceous siltstones of the Puncoviscana  
335 Formation (Zeballos et al. 2016, Do Campo and Nieto 2003). Kaolinite is stable under subaerial/near-  
336 surface conditions and is often correlated with temperate and humid paleoclimatic conditions (Do  
337 Campo et al. 2018).

338

### 339 **Paleontology**

340 The paleobotanical and palynological assemblage is diverse and consists of plants remains and pollen  
341 types that suggest a lake/marsh environment surrounded by woodland vegetation under humid  
342 conditions. The monolet spores of ferns described are characteristic of epiphytic Polyopodiaceae from  
343 the Yungas biogeographic region, predominant in the Selva Montana, a vegetation zone found on

344 eastern flanks of the NW Argentine Andes between 900 and 1,600 m a.s.l. with an average annual  
345 rainfall of up to 1,800 mm (Malizia et al. 2012).

346 The snails of the genus *Biomphalaria* documented in this study suggest the coeval existence of  
347 lentic, vegetated, and very shallow water bodies within lotic systems such as streams and rivers, with  
348 abundant submerged vegetation (De Francesco and Hassan 2009). The high degree of fragmentation  
349 and wear of the shells suggests an important taphonomic alteration, likely caused by sediment  
350 reworking. According to the sedimentological context, the lake environment would have been subject  
351 to episodic flows of water from the main fluvial system, i.e. the Río Toro. This situation would have  
352 promoted adverse conditions for the fossilization of the molluscs, which could have been subjected to  
353 reworking as well as bioturbation. Some recent taphonomic studies indicate that freshwater  
354 environments with the presence of abundant aquatic vegetation (and high concentrations of organic  
355 matter) significantly affect the preservation of molluscs, mainly through the dissolution of carbonate  
356 shells (De Francesco et al. 2020). The presence of various remains of indeterminable gastropod shells  
357 supports this interpretation.

358

### 359 **Geomorphological considerations**

360 As the concavity of the Río Toro changes at the confluence with the Río Capillas, it is likely that the  
361 additional discharge facilitates downstream sediment transport. Sediment entering the Río Toro north  
362 of the confluence does not seem to be transported as easily, leading to a rather convex stream profile.  
363 Indeed, a recent InSAR (synthetic aperture radar interferometry) study has shown that the landscape in  
364 this low-vegetated part of the valley is relatively unstable and susceptible to failure and the generation  
365 of debris flows (Olen et al. 2020). These findings are consistent with modern catchment-wide erosion  
366 rates from in situ-produced cosmogenic  $^{10}\text{Be}$ , which, in contrast to the drier and less steep northern  
367 sectors of the valley, document relatively high rates (approximately 1-1.5 mm/yr) and hillslope  
368 dominated sediment transport processes within tributary catchments in the southern part of the  
369 Quebrada del Toro (Bookhagen and Strecker 2012, Tofelde et al. 2018). Hence, in times of increased  
370 intermontane rainfall large amounts of debris may be generated and fed into the Río Toro, however,  
371 exporting this material may still be difficult, causing river damming. In fact, when projecting the 60 m  
372 high alluvial fan surface from the El Candado fan across the Quebrada del Toro suggests a prominent  
373 barrier to dam the Río Toro.

374

### 375 **Paleoclimatic considerations**

376 Since the middle Holocene lake/marsh episodes of El Candado may have been formed as a result of the  
377 development of the El Candado alluvial fans and the subsequent damming of the Toro River, the

378 question now arises as to the conditions that may have led to it.

379 The El Candado catchment is located along the western slopes of the tectonically active Sierra  
380 Pascha Sur and intersected by the Incamayo Fault (Fig. 2, Sánchez et al. 2010), therefore a tectonic  
381 control of alluvial fans in this area cannot be excluded. However, due to the lack of geological evidence,  
382 such as deformed layers or syn-sedimentary landslide deposits associated with the investigated  
383 outcrops, we consider this control to be insignificant and focus on the paleoclimatic conditions during  
384 the middle Holocene.

385 Based on our paleobotanical and palynological evidence, the studied sector of the Quebrada del  
386 Toro may have been relatively more humid during the middle Holocene (8.2 to 4.2 ka) than today. As  
387 a consequence, significant amounts of sediment must have been mobilized to give rise to the formation  
388 of thick alluvial fans with the potential to dam temporary lakes. This is especially true for areas with  
389 steep channel gradients such as those from our study area (Bookhagen and Strecker 2012, Tofelde et al.  
390 2018, Olen et al. 2020).

391 Although the Holocene of the Central Andes is considered relatively arid (Tchilinguirian and  
392 Morales 2013; and references therein), numerous studies have locally documented episodes of higher  
393 humidity during the last 10 ka (Morales and Schittek 2008, Morales 2011, Tchilinguirian et al. 2014,  
394 Alcalde and Kulemeyer 1999, Olivera et al. 2006, Tchilinguirian 2009, Betancourt et al. 2000, Rech et  
395 al. 2002, Latorre et al. 2006, Yacobaccio and Morales 2005). In northwestern Argentina, another  
396 sedimentary record of similar age and humid conditions (ca. 10-4 ka BP) is that of Lake El Rincón in  
397 the Tafi del Valle region (26.9°S; Garralla et al. 2001).

398 The described humid conditions during the middle Holocene may be related to dynamics of the  
399 South American Monsoon system and/or ENSO activity, which would have influenced the variability  
400 of precipitation during this period in northwestern Argentina (Zhou and Lau 2001, Grimm 2011,  
401 Novello et al. 2017, Montini et al. 2019).

402

## 403 CONCLUSIONS

404 In this study, we investigated the origin and evolution of late Quaternary lacustrine beds intercalated  
405 with alluvial fans deposits in the southern sector of the Quebrada del Toro (Eastern Cordillera, NW  
406 Argentina). Our results suggest that during the middle Holocene (ca. 8-4.8 ka BP) the development of  
407 large alluvial fans and the consequent damming of the Toro River created exclusively clastic lakes  
408 events.

409 Combined facies characteristics, paleontological content, and clay mineral compositions indicate  
410 that deposition took place in multiple temporary shallow lake-marsh environments with alkaline water  
411 under humid conditions. This suggests a wet period in an otherwise mainly dry area of northwestern

412 Argentina during the middle Holocene that may have been related to the dynamics of the SASM system,  
413 possibly influenced by ENSO activity. We suspect that these climatic conditions favored the  
414 mobilization of abundant coarse-grained sediments from adjacent steep mountain slopes, which  
415 provided the material for the construction of sufficiently large alluvial fans to dam the Río Toro.

416

#### 417 **Acknowledgements**

418 The authors wish to thank Prof. Alonso for insightful discussions and logistical support and Prof.  
419 Manfred R. Strecker and Dra. Stefanie Tofelde for sample collection of organic matter and constructive  
420 discussions. We acknowledge Dr. Francisco E. Córdoba (editor), Dr. Luis R. Horta, and an anonymous  
421 reviewer for their evaluations that improved the manuscript. In addition, the authors would like to thank  
422 Luis Veizaga for digitizing some of the illustrations and the CONICET and the Universidad Nacional  
423 de Salta for their financial support.

424

#### 425 **REFERENCES**

- 426 Alcalde, J.A. and Kulemeyer, J.J. 1999. The Holocene in the south-eastern region of the province Jujuy, northwest  
427 Argentina. *Quaternary International* 57-58: 13-116.
- 428 Álvarez, L.M., Sánchez, M.C. and Salfity, J.A. 2012. Los depósitos cuaternarios lacustres del tramo medio de la Quebrada  
429 del Toro, noroeste argentino. 13° Reunión Argentina de Sedimentología, Relatorio, p. 25-36. Salta.
- 430 Baker, P. and Fritz, S.C. 2015. Nature and causes of quaternary climate variation of tropical South America. *Quaternary*  
431 *Sciences Review* 124: 31–47.
- 432 Barnes, J. B., Ehlers, T. A., Insel, N., McQuarrie, N., & Poulsen, C. J. (2012). Linking orography, climate, and exhumation  
433 across the central Andes. *Geology* 40(12): 1135-1138.
- 434 Betancourt, J.L., Latorre, C., Rech, J.A., Quade, J. and Rylander, K. 2000. A 22,000-year record of monsoonal precipitation  
435 from northern Chile's Atacama Desert. *Science* 289: 1542-1546.
- 436 Biscaye, P. E. 1965. Mineralogy and sedimentation of recent deep-sea clay in the Atlantic Ocean and adjacent seas and  
437 oceans. *Geological Society of America Bulletin* 76(7): 803-832.
- 438 Blair, T. C. and McPherson, J. G. 1994. Alluvial fans and their natural distinction from rivers based on morphology,  
439 hydraulic processes, sedimentary processes, and facies assemblages. *Journal of Sedimentary Research* 64(3a): 450-489.
- 440 Blikra, L.H. and Nemeo, W. 1998. Postglacial colluvium in western Norway: depositional process, facies and paleoclimatic  
441 record. *Sedimentology* 45: 909-959.
- 442 Bobst, A.L., Lowenstein, T.K., Jordan, T.E., Godfrey, L.V., Ku, T. L. and Luo, S. 2001. A106 ka paleoclimate record from  
443 drill core of the Salar de Atacama, north-ern Chile. *Palaeogeography, Palaeoclimatology, Palaeoecology* 173: 21–42.
- 444 Bookhagen, B., Haselton, K. and Trauth, M. H. 2001. Hydrological modelling of a Pleistocene landslide-dammed lake in the  
445 Santa Maria Basin, NW Argentina. *Palaeogeography, Palaeoclimatology, Palaeoecology* 169(1-2): 113–127.
- 446 Bookhagen, B. and Strecker, M. R. 2008. Orographic barriers, high-resolution TRMM rainfall, and relief variations along  
447 the eastern Andes. *Geophysical Research Letters* 35(6).
- 448 Bookhagen, B. and Strecker, M. R. 2012. Spatiotemporal trends in erosion rates across a pronounced rainfall gradient:  
449 Examples from the southern Central Andes. *Earth and Planetary Science Letters* 327: 97-110.
- 450 Bronk Ramsey, C. 2001. Development of the radiocarbon calibration program. *Radiocarbon*, 43(2A), 355-363.
- 451 Castino, F., Bookhagen, B. and Strecker, M.R. 2016. Rainfall variability and trends of the past six decades (1950–2014) in  
452 the subtropical NW Argentine Andes. *Climatic Dynamics* 1–19.

- 453 Chamley, H. 1997. Clay mineral sedimentation in the ocean. In: Soil and sediment. Springer-Verlag, 269-302, Berlin.
- 454 Collinson, J. D. 1978. Lakes. *Sedimentary Environments and Facies*, 61, 79.
- 455 Collinson, J. D. and Thompson, D. B. 1989. *Sedimentary Structure* (2nd ed.). Uniwin Hyman, London.
- 456 Colombo, F. 2005. Quaternary telescopic-like alluvial fans, Andean Range, Argentina, en Harvey, A.M., Mather, A.E. y  
457 Stockes, M. (eds.), *Alluvial Fans: Geomorphology, Sedimentology Dynamics*. Geological Society, Special Publications,  
458 251: 69-84.
- 459 Colombo, F., Limarino, C., Busquets, P., Solé de Porta, N., Heredia, N., Rodríguez-Fernández, R. and Alvarez-Marron, J.  
460 2005. Primeras edades absolutas de los depósitos lacustres holocenos del río Jáchal, Precordillera de San Juan. *Revista*  
461 *de la Asociación Geológica Argentina* 60(3): 606-608.
- 462 Colombo, F., Limarino, C., Busquets, P., Solé de Porta, N., Heredia, N., Rodríguez-Fernández, R. and Alvarez-Marron, J.  
463 2009. Holocene intramontane lake development: A new model in the Jáchal River Valley, Andean Precordillera, San  
464 Juan, Argentina. *Journal of South American Earth Sciences* 28: 229-238.
- 465 Coussot, P. and Meunier, M. 1996. Recognition, classification and mechanical description of debris flows. *Earth Sciences*  
466 *Reviews* 40: 209-227.
- 467 De Francesco, C. G., Zárate, M. A. and Miquel, S. E. 2007. Late Pleistocene mollusc assemblages and inferred  
468 paleoenvironments from the Andean piedmont of Mendoza, Argentina. *Palaeogeography, Palaeoclimatology,*  
469 *Palaeoecology* 251(3-4), 461-469.
- 470 De Francesco, C.G. and Hassan, G.S. 2009. The significance of molluscs as paleoecological indicators of freshwater system  
471 in central-western Argentina. *Palaeogeography, Palaeoclimatology, Palaeoecology* 274: 105-113.
- 472 De Francesco, C. G., Tietze, E., Cristini, P. A. and Hassan, G. S. 2020. Actualistic taphonomy of freshwater molluscs from  
473 the Argentine Pampas: an overview of recent research progress. In: S. Martínez, A. Rojas, F. Cabrera (eds.), *Actualistic*  
474 *Taphonomy in South America*. Springer Nature Switzerland AG 2020. *Topics in Geobiology* 48: 69-88.
- 475 Do Campo, M. and Nieto, F. 2003. Transmission electron microscopy study of very low-grade metamorphic evolution in  
476 Neoproterozoic pelites of the Puncoviscana formation (Cordillera Oriental, NW Argentina). *Clay Minerals* 38(4): 459-  
477 481.
- 478 Do Campo, M., Bauluz B., Del Papa C., White T., Yuste A. and Mayayo M.J. 2018. Evidence of cyclic climatic changes  
479 recorded in clay mineral assemblages from a continental Paleocene-Eocene sequence, northwestern Argentina.  
480 *Sedimentary Geology* 368: 44-57.
- 481 Fregenal Martínez, M. A., Meléndez, N. and Arche, A. 2010. Lagos y sistemas lacustres. *Sedimentología. Del Proceso*  
482 *Físico a la Cuenca Sedimentaria*: Madrid, Consejo Superior de Investigaciones Científicas, 299-395.
- 483 Fritz, S.C., Baker, P.A., Ekdahl, E., Seltzer, G.O. and Stevens, L.R. 2010. Millennial-scale climate variability during the Last  
484 Glacial period in the tropical Andes. *Quat. Sci. Rev.* 29: 1017-1024.
- 485 Fritz, S.C., Baker, P.A., Lowenstein, T.K., Seltzer, G.O., Rigsby, C.A., Dwyer, G.S., Tapia, P.M., Arnold, K.K., Ku, T.L.  
486 and Luo, S. 2004. Hydrologic variation during the last 170,000 years in the southern hemisphere tropics of South  
487 America. *Quaternary Research* 61: 95-104.
- 488 Garralla, S., Muruaga, C. and Herbst, R. 2001. Lago El Rincón, Holoceno del Departamento de Tañ del Valle, Provincia de  
489 Tucumán (Argentina): palinología y facies sedimentarias. *Ameghiniana* 8: 91-99 (Publicación Especial).
- 490 Grimm, A. M. 2011. Interannual climate variability in South America: Impacts on seasonal precipitation, extreme events,  
491 and possible effects of climate change. *Stochastic Environmental Research and Risk Assessment*, 25(4): 537-554.
- 492 Godfrey, L.V., Jordan, T.E., Lowenstein, T.K. and Alonso, R.L. 2003. Stable isotope constraints on the transport of water to  
493 the Andes between 22° and 26°S during the last glacial cycle. *Palaeogeography, Palaeoclimatology, Palaeoecology* 194:  
494 299-317.
- 495 Gutiérrez, F., Gutiérrez, M. and Sancho, C. 1988. Geomorphological and sedimentological analysis of a catastrophic flash  
496 flood in the Arás drainage basin (Central Pyrenees, Spain). *Geomorphology*, 22: 265-283.
- 497 Gutiérrez Elorza, M. 2001. *Geomorfología Climática*. Ediciones Omega, 642 p. Barcelona.
- 498 Hermanns, R. L. and Strecker, M. R. 1999. Structural and lithological controls on large Quaternary rock avalanches  
499 (sturzstroms) in arid northwestern Argentina. *Geological Society of America Bulletin* 111(6): 934-948.
- 500 Hermanns, R. L., Niedermann, S., Ivy-Ochs, S. and Kubik, P. W. 2004. Rock avalanching into a landslide-dammed lake  
501 causing multiple dam failure in Las Conchas valley (NW Argentina)—evidence from surface exposure dating and  
502 stratigraphic analyses. *Landslides* 1(2): 113-122.

- 503 Hogg, A., Heaton, T., Hua, Q., Palmer, J., Turney, C., Southon, J., Bayliss, A., Blackwell, P., Boswijk, G., Bronk Ramsey,  
504 C., Petchey, F., Reimer, P., Reimer, R., & Wacker, L. 2020. SHCal20 Southern Hemisphere calibration, 0–55,000 years  
505 cal BP. *Radiocarbon* 62(4): 759-778.
- 506 Kilmurray, J. and Igarzábal, A. 1971. Petrografía y rasgos geomórficos del batolito granítico de Santa Rosa de Tastil,  
507 provincia de Salta, Rep. Argentina. *Revista de la Asociación Geológica Argentina* 26(4): 417-438.
- 508 Latorre, C., Betancourt, J.L. and Arroyo, T.K. 2006. Late Quaternary vegetation and climate history of a perennial river  
509 canyon in the Río Salado basin (22°S) of Northern Chile. *Quaternary Research* 65: 450-466.
- 510 Malizia, L., Pacheco, S., Blundo, C. and Brown, A. D. 2012. Caracterización altitudinal, uso y conservación de las Yungas  
511 Subtropicales de Argentina. *Revista Ecosistemas* 21(1-2): 53-73.
- 512 Markgraf, V., Bradbury, J.P. and Fernández, J. 1986. Bajada de Rahue, province of Neuquen, Argentina: An interstadial  
513 deposit in northern Patagonia. *Palaeogeography, Palaeoclimatology, Palaeoecology* 56: 51-258.
- 514 Markgraf, V. and Seltzer, G. O. 2001. Pole-Equator-Pole paleoclimates of the Americas integration: toward the big picture.  
515 In: Markgraf, V., (ed.) *Interhemispheric Climate Linkages*. Academic Press, San Diego, CA, 433-442.
- 516 Marrett, R. A., Allmendinger, R. W., Alonso, R. N. and Drake, R. E. 1994. Late Cenozoic tectonic evolution of the Puna  
517 Plateau and adjacent foreland, northwestern Argentine Andes. *Journal of South American Earth Sciences* 7(2): 179-207.
- 518 Marquillas, R. A., Del Papa, C. and Sabino, I. F. 2005. Sedimentary aspects and paleoenvironmental evolution of a rift basin:  
519 Salta Group (Cretaceous–Paleogene), northwestern Argentina. *International Journal of Earth Sciences* 94(1): 94-113.
- 520 May, J. H. and Soler, R. D. 2011. Late Quaternary morphodynamics in the Quebrada de Purmamarca, NW Argentina. *E&G  
521 Quaternary Science Journal* 59(1-2) : 21-35.
- 522 Mazzuoli, R., Vezzoli, L., Omarini, R., Acocella, V., Gioncada, A., Matteini, M., Dini, A., Guillou, H., Hauser, N., Uttini,  
523 A. and Scaillet, S. 2008. Miocene magmatism and tectonics of the easternmost sector of the Calama–Olacapato–El Toro  
524 fault system in Central Andes at ~ 24 S: Insights into the evolution of the Eastern Cordillera. *Geological Society of  
525 America Bulletin* 120(11-12): 1493-1517.
- 526 Miall, A.D., 1996. *The Geology of Fluvial Deposits: Sedimentary Facies, Basin Analysis, and Petroleum Geology*. Springer-  
527 Verlag, 582 p., Berlin.
- 528 Molina, J.I. 2006. Estratigrafía de los depósitos volcanoclasticos neógenos entre Ingeniero Maury y San Bernardo de las  
529 Zorras, quebrada del Toro, Salta. Universidad Nacional de Salta, Tesis Profesional, 202 p., Salta.
- 530 Montini, T. L., Jones, C. and Carvalho, L. M. 2019. The South American low-level jet: A new climatology, variability, and  
531 changes. *Journal of Geophysical Research: Atmospheres*, 124(3): 1200-1218.
- 532 Moore, D.M. and Reynolds Jr., R.C. 1997. *X-ray diffraction and the identification and analysis of clay minerals*. Oxford  
533 University Press, 332 p., Oxford.
- 534 Morales, M.R. 2011. Arqueología ambiental del Holoceno Temprano y medio en la Puna Seca Argentina. Modelos  
535 paleoambientales multi-escalas y sus implicancias para la arqueología de cazadores-recolectores. In: *British  
536 Archaeological Research* 2295, South American Archaeology Series, vol. 15. Archaeopress, Oxford, UK.
- 537 Morales, M. and Schitteck, K. 2008. Primeros resultados paleoambientales del Holoceno medio en Alto Tocomar (Puna  
538 Salteña): interpretación local e implicancias regionales. In: *Primeras jornadas del área puneña de los Andes Centro-Sur,  
539 Tucumán, Argentina*, 109-110.
- 540 Novello, V. F., Cruz, F. W., Vuille, M., Strikis, N. M., Edwards, R. L., Cheng, H., Emerick, S., de Paula, M. S., Li, X.,  
541 Barreto E. de S., Karmann, I. and Santos, R. V. 2017. A high-resolution history of the South American Monsoon from  
542 Last Glacial Maximum to the Holocene. *Scientific reports* 7(1): 1-8.
- 543 Olen, S. and Bookhagen, B. 2020. Applications of SAR Interferometric Coherence Time Series: Spatiotemporal Dynamics  
544 of Geomorphic Transitions in the South-Central Andes. *Journal of Geophysical Research: Earth Surface* 125(3).
- 545 Olivera, D.E., Tchilinguirian, P. and De Aguirre, M.J. 2006. Cultural and Environmental Evolution in the Meridional Sector  
546 of the Puna of Atacama during the Holocene. In: *International Prehistoric Congress. En Change in the Andes: Origins of  
547 Social Complexity Pastoralism and Agriculture*. Acts of the 14° UISPP Congress. University of Liege, Belgium. 1-7.
- 548 Pierce, J. W. and Siegel F.R. 1969. Quantification in clay mineral studies of sediments and sedimentary rocks. *Journal of  
549 Sedimentary Research* 39(1): 187-193.
- 550 Pingel, H., Strecker, M. R., Alonso, R. N. and Schmitt, A. K. 2013. Neotectonic basin and landscape evolution in the Eastern  
551 Cordillera of NW Argentina, Humahuaca Basin (~ 24 S). *Basin Research* 25(5): 554-573.
- 552 Pingel, H., Strecker, M. R., Mulch, A., Alonso, R. N., Cottle, J. and Rohrmann, A. 2020. Late Cenozoic topographic

- 553 evolution of the Eastern Cordillera and Puna Plateau margin in the southern Central Andes (NW Argentina). *Earth and*  
554 *Planetary Science Letters* 535.
- 555 Piovano E., Córdoba, F. y Stutz, S. 2014. Limnogeology in Southern South America: an overview. *Latin American Journal*  
556 *of Sedimentology and Basin Analysis* 21 (2): 65-75.
- 557 Placzek, C., Quade, J. and Patchett, P.J. 2006. Geochronology and stratigraphy of late Pleistocene lake cycles on the  
558 southern Bolivian Altiplano: implications for causes of tropical climate change. *Geology Society American Bulletin*  
559 118: 515-532.
- 560 Rech, J. A., Quade, J. and Betancourt, J. L. 2002. Late Quaternary paleohydrology of the central Atacama Desert (lat 22-24  
561 S), Chile. *Geological Society of America Bulletin* 114(3): 334-348.
- 562 Robinson, R. A. J., Spencer, J. Q. G., Strecker, M. R., Richter, A. and Alonso, R. N. 2005. Luminescence dating of alluvial  
563 fans in intramontane basins of NW Argentina. *Alluvial Fans: Geomorphology, Sedimentology, Dynamics* 251: 152-  
564 168.
- 565 Sánchez, M.C., Caba, R.E. and Salfity, J.A. 2010. Geología Ambiental del tramo inferior de la Quebrada del Toro,  
566 provincial de Salta. *Revista de Geología Aplicada a la Ingeniería y al Ambiente* 25: 77-88.
- 567 Sánchez, M.C., Lucena, L.L., Rivelli, F.R. and Salfity, J.A. 2005. Geología y geomorfología de la cuenca del río Pascha-  
568 Incamayo, Quebrada del Toro, Salta. 16° Congreso Geológico Argentino, Actas 3: 529-536, La Plata.
- 569 Savi, S., Schildgen, T. F., Tofelde, S., Wittmann, H., Scherler, D., Mey, J., Alonso R.N. and Strecker, M.R. 2016. Climatic  
570 controls on debris-flow activity and sediment aggradation: The Del Medio fan, NW Argentina. *Journal of Geophysical*  
571 *Research* 1-22.
- 572 Schultz, L. G. 1964. Quantitative interpretation of mineralogical composition from X-ray and chemical data for the Pierre  
573 Shale. *US Geological Survey of Professionals. Papers*, 391-C.
- 574 Schwanghart, W. and Kuhn, N. J. 2010. TopoToolbox: A set of Matlab functions for topographic analysis. *Environmental*  
575 *Modelling & Software* 25(6): 770-781.
- 576 Sobel, E. R. and Strecker, M. R. 2003. Uplift, exhumation and precipitation: tectonic and climatic control of Late Cenozoic  
577 landscape evolution in the northern Sierras Pampeanas, Argentina. *Basin Research* 15(4): 431-451.
- 578 Spalletti, L.A. 2001. Modelo de sedimentación fluvial y lacustre en el margen pasivo de un hemigraben: el Triásico de la  
579 Precordillera occidental de San Juan, República Argentina. *Revista de la Asociación Geológica Argentina* 56(2): 189-  
580 210.
- 581 Strecker, M. R., Alonso, R. N., Bookhagen, B., Carrapa, B., Hilley, G. E., Sobel, E. R. and Trauth, M. H. 2007. Tectonics  
582 and climate of the southern central Andes. *Annual Reviews Earth Planetary Sciences* 35: 747-787.
- 583 Suriano, J. and Limarino, C.Q. 2009. Sedimentación pedemontana en las nacientes del río Jachal y Pampa de Gualilán,  
584 Precordillera de San Juan. *Revista de la Asociación Geológica Argentina* 65(3): 516-532.
- 585 Tchilinguirian, P. 2009. Paleoambientes Holocenos en la Puna Austral (27°S): implicancias geoarqueológicas, Argentina.  
586 Tesis doctoral, Universidad de Buenos Aires (inédita), Buenos Aires.
- 587 Tchilinguirian, P. and Morales, M. R. 2013. Mid-Holocene paleoenvironments in Northwestern Argentina: Main patterns  
588 and discrepancies. *Quaternary International* 307: 14-23.
- 589 Tchilinguirian, P., Morales, M. R., Oxman, B., Lupo, L. C., Olivera, D. E. and Yacobaccio, H. D. 2014. Early to Middle  
590 Holocene transition in the Pastos Chicos record, dry Puna of Argentina. *Quaternary international* 330: 171-182.
- 591 Tiner, R. J., Negrini, R. M., Antinao, J. L., McDonald, E. and Maldonado, A. 2018. Geophysical and geochemical  
592 constraints on the age and paleoclimate implications of Holocene lacustrine cores from the Andes of central Chile.  
593 *Journal of Quaternary Science* 33(2): 150-165.
- 594 Tofelde, S., Schildgen, T. F., Savi, S., Pingel, H., Wickert, A. D., Bookhagen, B., Wittmann, H., Alonso, R.N., Cottle, J. and  
595 Strecker, M. R. 2017. 100 kyr fluvial cut-and-fill terrace cycles since the Middle Pleistocene in the southern Central  
596 Andes, NW Argentina. *Earth and Planetary Science Letters* 473: 141-153.
- 597 Tofelde, S., Duesing, W., Schildgen, T. F., Wickert, A. D., Wittmann, H., Alonso, R. N. and Strecker, M. 2018. Effects of  
598 deep-seated versus shallow hillslope processes on cosmogenic <sup>10</sup>Be concentrations in fluvial sand and gravel. *Earth*  
599 *Surface Processes and Landforms* 43(15): 3086-3098.
- 600 Trauth, M. H., Alonso, R. A., Haselton, K. R., Hermanns, R. L. and Strecker, M. R. 2000. Climate change and mass  
601 movements in the NW Argentine Andes. *Earth and Planetary Science Letters* 179(2): 243-256.
- 602 Trauth, M.H., Bookhagen, B., Marwan, N. and Strecker, M. 2003. Multiple Landslides clusters record Quaternary climate



- 603 change in the NW Argentine Andes. *Paleogeography, Palaeoclimatology, Palaeoecology* 194: 109-121.
- 604 Turner, J.C.M. 1960. Estratigrafía de la sierra de Santa Victoria y adyacencias. *Boletín de la Academia Nacional de Ciencias*  
605 de Córdoba 41(2): 163-196.
- 606 Veizaga Saavedra, J.G. 2012. Los abanicos aluviales cuaternarios de la Quebrada del Toro, noroeste argentino: tramo  
607 inferior y medio. Tesis Profesional, Universidad Nacional de Salta (inédita), 126 p., Salta.
- 608 Vera, C., Higgins, W., Amador, J., Ambrizzi, T., Garraud, R., Gochis, D., Gutzler, D., Lettenmaier, D., Marengo, J.,  
609 Mechoso, C.R., Nogues-Paegle, J., Silva Dias, P.L. and Zhang, C. 2006. Toward a unified view of the American  
610 monsoon systems. *Journal of climate* 19(20): 4977-5000.
- 611 Vezzoli, L., Acocella, V., Omarini, R. and Mazzuoli, R. 2012. Miocene sedimentation, volcanism and deformation in the  
612 Eastern Cordillera (24° 30' S, NW Argentina): tracking the evolution of the foreland basin of the Central Andes. *Basin*  
613 *Research* 24(6): 637-663.
- 614 Vezzoli, L., Matteini, M., Hauser, N., Omarini, R., Mazzuoli, R. and Acocella, V. 2009. Non-explosive magma-water  
615 interaction in a continental setting: Miocene examples from the Eastern Cordillera (central Andes; NW Argentina).  
616 *Bulletin of volcanology* 71(5): 509-532.
- 617 Villagrán, C. and Varela, J. 1990. Palynological evidence from increased aridity on the central Chilean coast during the  
618 Holocene. *Quaternary Research* 34: 198-207.
- 619 Villa Martínez, R., Villagrán, C. and Jenny, B. 2003. The last 7500 cal yr B.P. of westerly rainfall in Central Chile inferred  
620 from high-resolution pollen record from Laguna Aculeo (34°S). *Quaternary Research* 60: 284-293.
- 621 Yacobaccio, H. D. and Morales, M. 2005. Mid-Holocene environment and human occupation of the Puna (Susques,  
622 Argentina). *Quaternary International* 132(1): 5-14.
- 623 Wayne, W.J. 1999. The Alemania rockfall dam: a record of Mid-Holocene earthquake and catastrophic flood in  
624 northwestern Argentina. *Geomorphology* 27: 295-306.
- 625 Zeballos, A., Weihed P., Blanco M. and Machaca V. 2016. Geological, mineralogical and chemical characterization of  
626 Devonian kaolinite-bearing sediments for further applications in the ceramic (tiles) industry in La Paz, Bolivia.  
627 *Environmental Earth Sciences* 75(7): 546.
- 628 Zhou, J. and Lau, K. M. 2001. Principal modes of interannual and decadal variability of summer rainfall over South  
629 America. *International Journal of Climatology*, 21(13): 1623-1644.
- 630
- 631

632 **TABLES**

633 Table 1. Lithofacies described for fluvial, alluvial, and lacustrine deposits of the  
634 Quebrada del Toro.

635

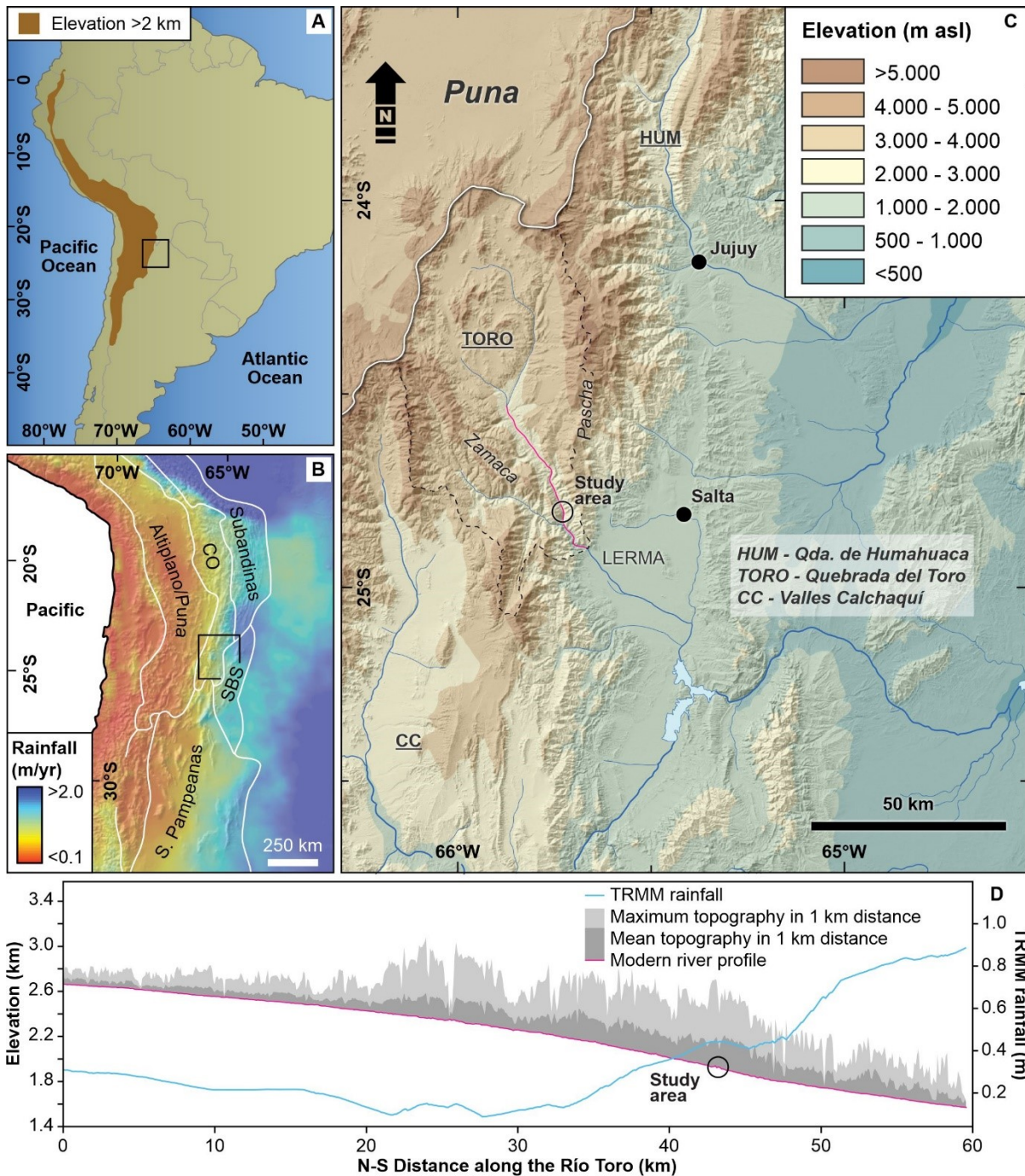
636 Table 2. Calibrated  $^{14}\text{C}$  ages and sample locations

637

638

MANUSCRITO ACEPTADO

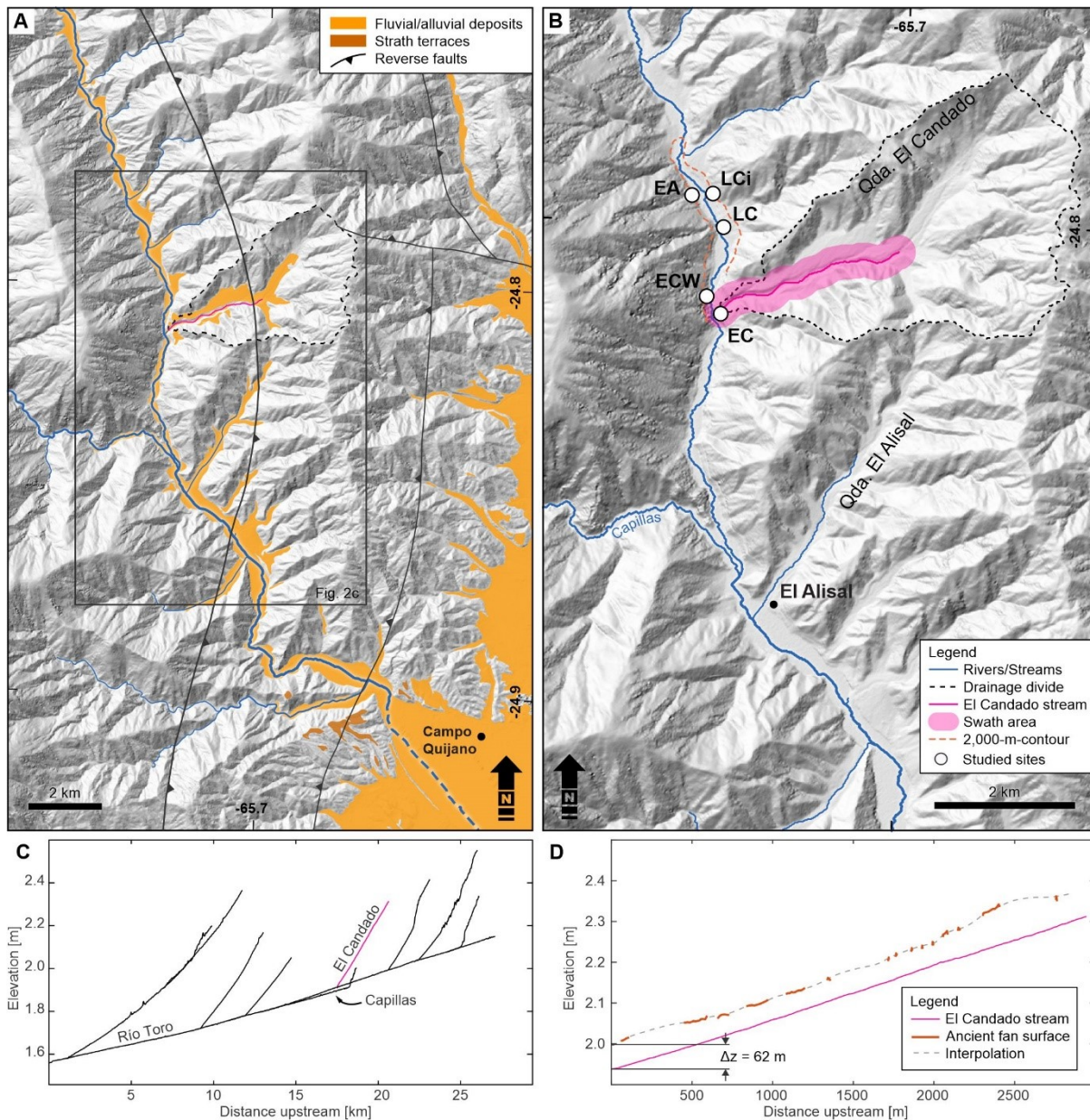
639 FIGURE CAPTIONS



640

641 **Figure 1.** a) Overview map of South America showing Andean topography (>2 km a.s.l.) and extent of  
 642 Fig. 1c (black box). b) Morphotectonic map of southern Central Andes showing mean annual rainfall  
 643 derived from NASA's (National Aeronautics and Space Administration) TRMM mission (Tropical  
 644 Rainfall Measurement Mission) and extent of Fig. 1c (black box). EC—Eastern Cordillera, SFTB—  
 645 Subandean fold-and-thrust belt; SBS—Santa Bárbara System. c) Digital elevation model of the southern  
 646 central Andes of NW Argentina (extracted from 90 m SRTM elevation data) showing the intermontane

647 Quebrada del Toro (dashed outline), adjacent sedimentary basins, and their drainage systems. A bold  
 648 white line delineates the internally drained Puna Plateau from the externally drained areas of the Andes.  
 649 d) Longitudinal river profile of the Río Toro (magenta line in Fig. 1c) showing the annual mean rainfall  
 650 amounts (from NASA-TRMM), the modern river profile, and the mean and maximum topography  
 651 within 1-km distance along the river. (a-c) modified from Pingel et al. (2020)  
 652



653 **Figure 2.** a) Shaded relief map from the southern sector of the Quebrada del Toro showing river network  
 654 and flat topography (slope  $\leq 15^\circ$ ) mainly associated with late Quaternary fluvial/alluvial lithologies  
 655 (using TanDEM-X-Digital Elevation Model, 12 m); b) Longitudinal river profiles of the lower reach of  
 656 the Río Toro and its tributaries. Studied sections: EA-El Alto, LCi-La Cirila, ECW-El Candado West,  
 657

658 and EC-El Candado; c) Shaded relief map of the El Candado area showing sampling locations, the El  
659 Candado catchment, and an upstream 2,000-m contour line; d) Longitudinal profile of the modern El  
660 Candado stream and the maximum elevation of the adjacent low relief surface, i.e. ancient alluvial fan  
661 surface (within 250 m distance). Note the elevation difference between the fan surface and the modern  
662 stream (62 m).

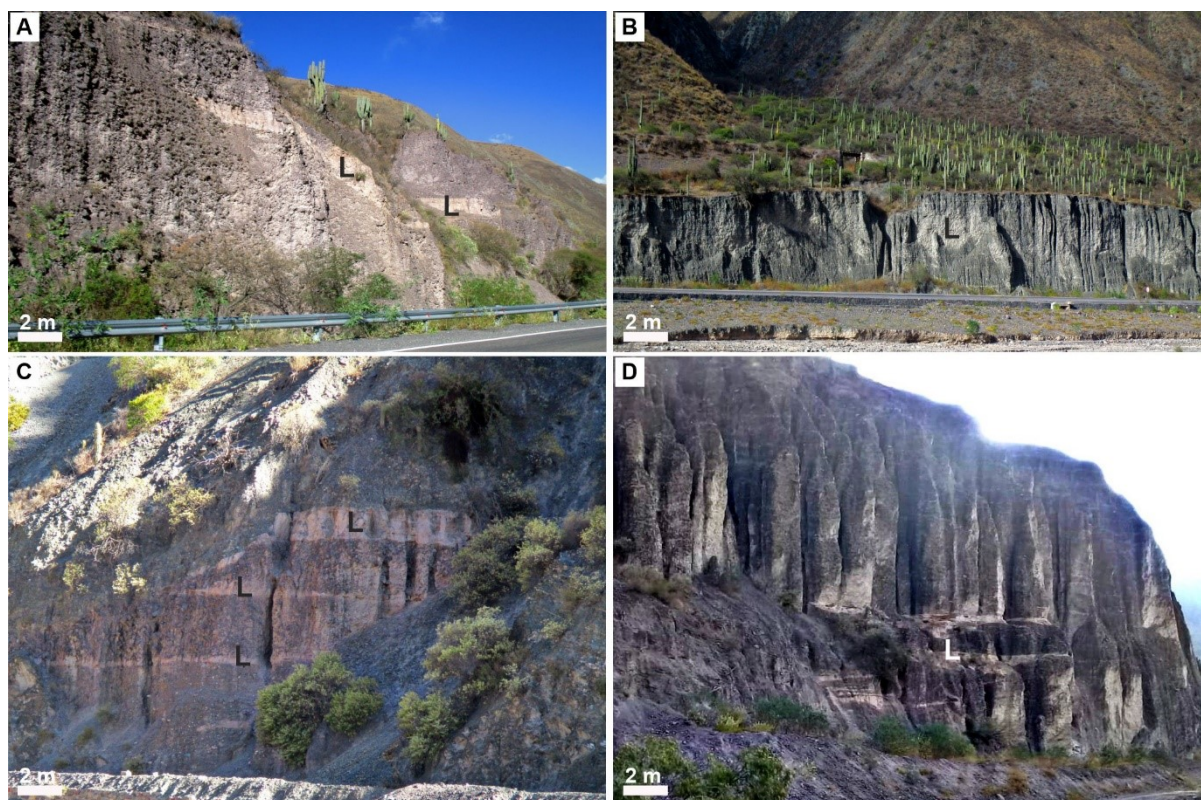
663



664

665 **Figure 3.** Oblique view to the north along the basement gorge of the Quebrada del Toro (Google Earth)  
666 illustrating the field relationship between the El Candado catchment area (outlined with dashed white  
667 line), its incised vestiges of the ancient El Candado alluvial fan (Ecaf, the surface is shown in orange),  
668 the location of stratigraphic sections, and the south draining Río Toro. The dashed orange line is a  
669 2,000-m contour line representing the upstream projection of the fan surface, i.e. the maximum possible  
670 extent of a dammed paleolake.

671



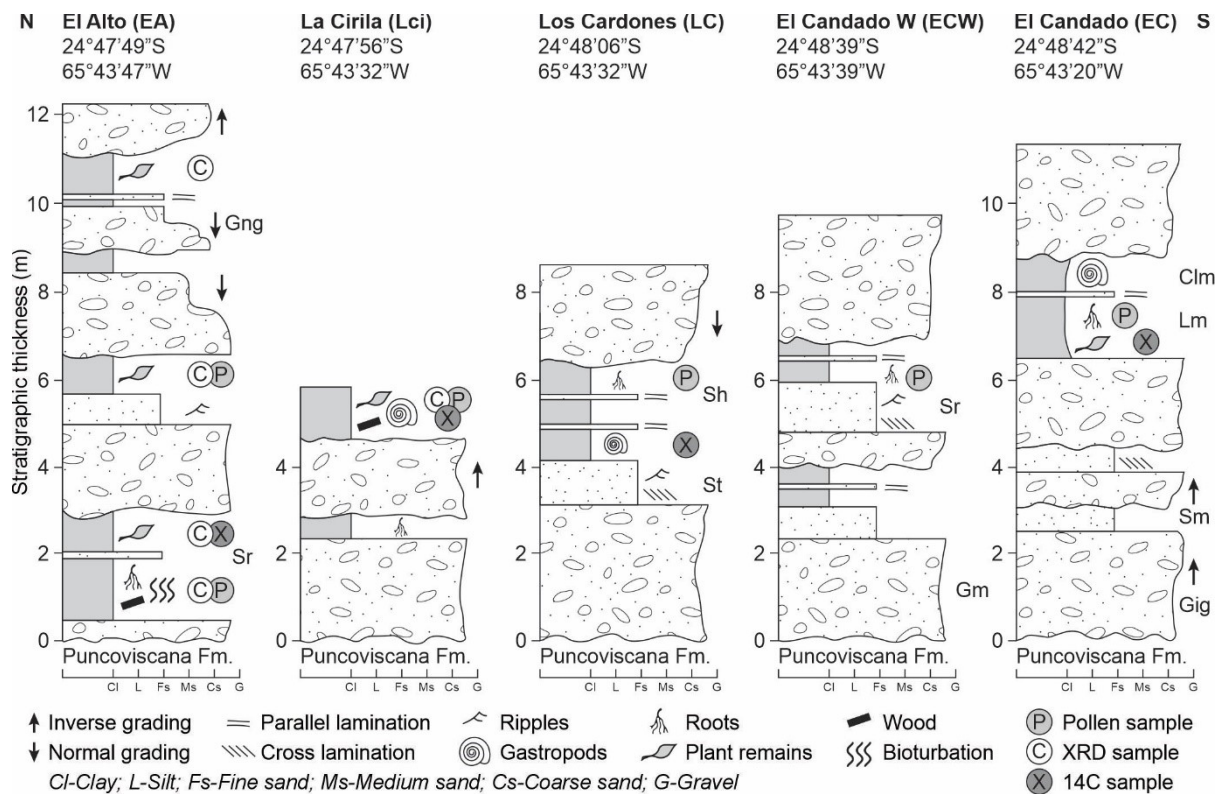
672

673 **Figure 4.** Field photographs of alluvial-fluvial deposits interdigitated with the lake deposits at the  
674 studied sites: a) El Candado; b) Los Cardones; c) El Candado West; d) El Alto. The tabular and/or  
675 lenticular levels of lighter color correspond to lacustrine beds (L).

676

677

MANUSCRITO

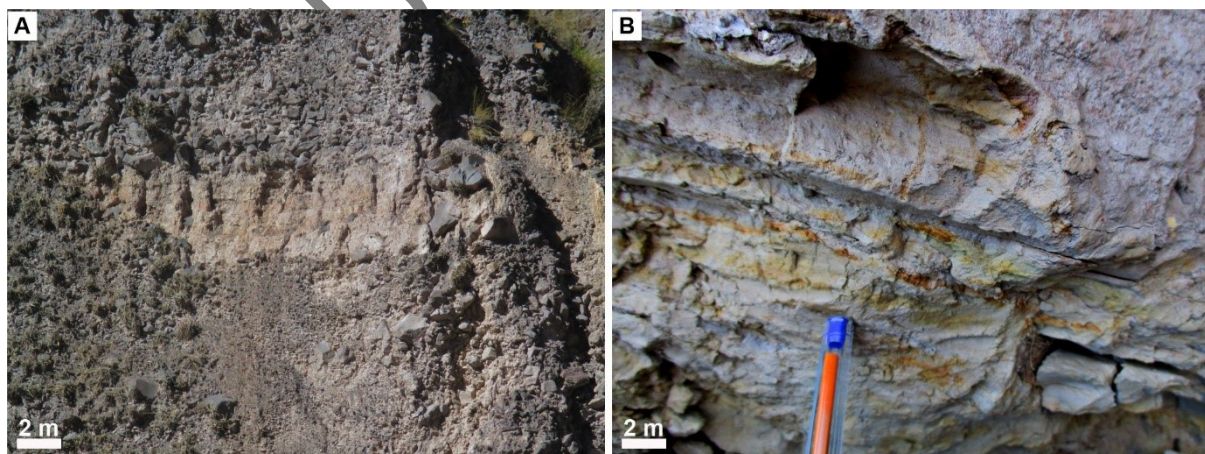


678

679

680 **Figure 5.** Measured stratigraphic sections of alluvial/lacustrine sections exposed along the Río Toro in  
 681 the El Candado area, showing additional paleontological and sedimentological information, as well as  
 682 sampling locations for our AMS <sup>14</sup>C geochronology, pollen, and geochemical analyses. Locations are  
 683 shown in Figures 2 and 3.

684

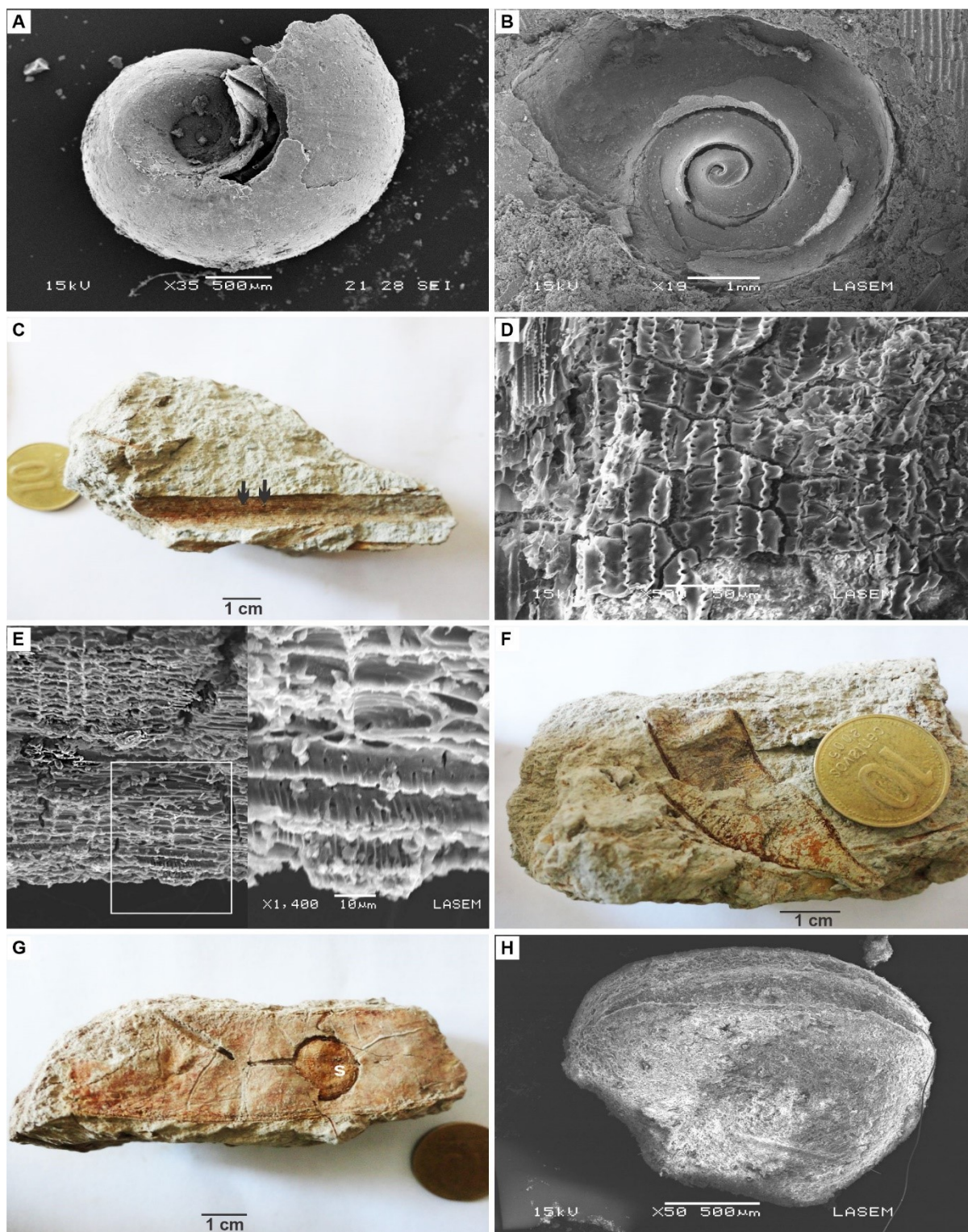


685

686 **Figure 6.** a) Massive lacustrine deposits (C1m) of the El Candado section concerning fluvial facies (SM  
 687 - massive sand and ST - sand with cross-lamination) and alluvial (Gm - massive gravel and Ggn - gravel  
 688 with normal gradation); b) Massive clay facies (C1m) with plant remains and with very fine levels of

689 charred plant remains (indicated by the white arrow) from the El Alto section.

690



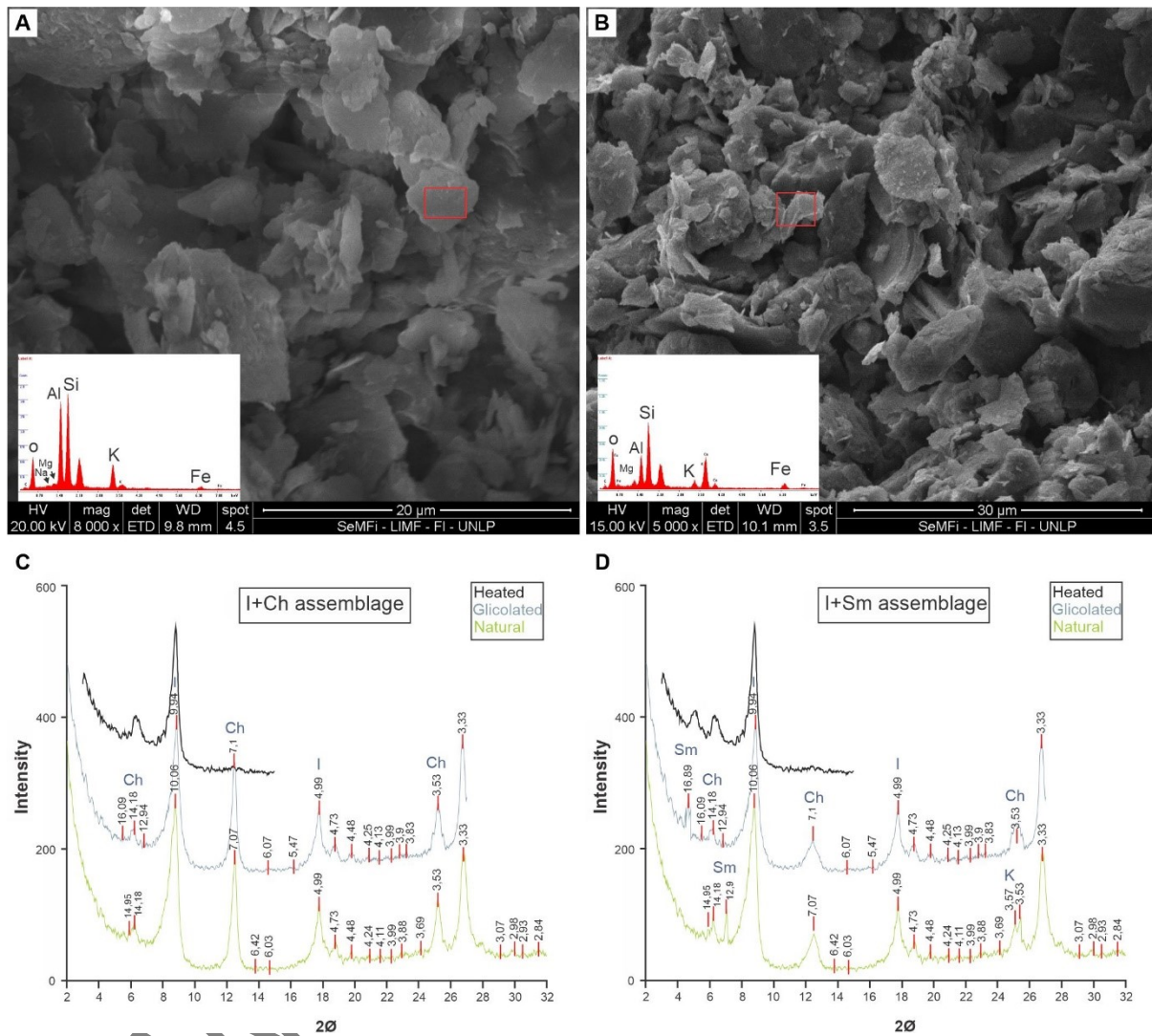
691

692 **Figure 7.** a-b) SEM images of *Biomphalaria* sp. from the lacustrine beds of the La Cirila section; c-f)

693 Plant remains samples of the La Cirila section; c) Hand sample of sandy/clay unit containing grass leaf



694 with stomata (arrows); d) SEM image of the epidermis of a grass leaf; e) Dicot stem with detail of  
695 conduction tissue; f) Fruit, legume type; g) Fruit showing legume seed; h) Legume seed.  
696



697  
698 **Figure 8.** a-b) SEM microphotographs and EDS results from middle Holocene lake deposits of the  
699 studied sections. a) Illite: high fragmented clays with variable size, irregular borders, without a  
700 preferential order. b) Smectite: curled flakes with open-air voids having small interfacial zones, flaky  
701 particle morphology. The red area indicates the area measured by EDS analysis of major elements. c-  
702 d) X-ray diffractograms of (c) illite+chlorite (I+Ch) and (d) illite+smectite (I+Sm) assemblages.

703  
704  
705  
706

707 **TABLES**

708 Table 1. Lithofacies described for fluvial, alluvial, and lacustrine deposits of the southern sector of the  
709 Quebrada del Toro.

<b>Lithofacies code</b>	<b>Description</b>	<b>Interpretation</b>
Gmc and Gm	Coarse gravel, clast-support (Gmc) and matrix-support (Gm), with silty sand to silt-clay matrix. Poor selection. Composed exclusively by angular and subangular clasts of the Puncoviscana Fm. With poorly defined tabular and lenticular stratification, with planar and erosive bases. Massive.	Debris flow with high kinetic energy, high viscosity, high density, with tractional transport.
Ggi	Fine gravel, matrix-support, with inverse gradation. Thin tabular beds.	Intermediate flows, between hyperconcentrates and fluids based on high availability and the slopes of the alluvial fans.
Gng	Medium gravel, matrix-support, with normal gradation. Medium tabular beds.	High energy, high density and high viscosity debris streams.
Sm	Medium to fine sandstone, grayish-brown. Planar-based tabular beds. Massive.	Sheet-flood, unconfined ephemeral streams.
St	Medium sandstone, brown to gray. With low angle planar cross lamination	Migration of small sand waves (2D type).
Sr	Fine sandstone, brown to yellowish-brown. Ripple lamination.	High flow rate stream.
Sh	Fine, grayish-brown sandstone. Thin tabular layers with parallel lamination.	High rate flows in planar bed phases associated with near supercritical high rate flows in response to laminar flood periods.
Am	Yellowish-brown clays. Tabular beds of 2 to 0.5 m thick. Massive. With desiccation cracks. With remains of gastropod shells, plant remains and bioturbation.	Very low energy lake deposit with periods of subaerial exposure.
Lm	Yellowish-brown silts. Massive.	Deposit generated by suspension-fallout in marginal positions of a body of water.

710

711

712 Table 2. Calibrated <sup>14</sup>C ages and sample locations

<b>Sample</b>	<b>Site</b>	<b>Material</b>	<b>Lab ID</b>	<b>Latitude</b>	<b>Longitude</b>	<b><sup>14</sup>C age ± 1σ (yr BP)</b>	<b><sup>14</sup>C age ± 1σ (cal yr BP)*</b>
QT-02032014-01	El Alto	Charcoal	Poz-63278	-24.797976	-65.729083	4790 ± 40	5480 ± 80
QT-02032014-02	El Alto	Charcoal	Poz-63279	-24.797976	-65.729083	4825 ± 35	5520 ± 60
ST14-46-C14	El Alto	Charcoal	Poz-63435	-24.798120	-65.729020	8030 ± 60	8840 ± 110
ST14-47-C14	El Alto	Organic matter	Poz-63283	-24.797590	-65.729080	7420 ± 80	8190 ± 100
Gastropods Toro	La Cirila	Gastropod shells	Poz-62843	-24.799011	-65.725642	6440 ± 40	7330 ± 60

\*converted from conventional ages using OxCal v4.4.3 (Bronk Ramsey 2001) and the SHCal 20 calibration data (Hogg et al. 2020).

713

714

715